sciendo

Int. J. of Applied Mechanics and Engineering, 2019, vol.24, No.4, pp.36-52
DOI: 10.2478/ijame-2019-0048

EFFECTS OF NON-UNIFORM HEAT GENERATION /ABSORPTION AND RADIATION ON HYDROMAGNETIC DISSIPATIVE FLOW OVER A POROUS NONLINEAR STRETCHING SURFACE WITH HEAT AND MASS FLUXES

S.P. ANJALI DEVI
Department of Applied Mathematics, Bharathiar University
Coimbatore - 641 046, TamilNadu, INDIA
E- mail: anjalidevi_s_p@yahoo.co.in

M. AGNEESHWARI*
Department of Mathematics
Sri Shakthi Institute of Engineering and Technology
Coimbatore-641062, TamilNadu, INDIA
E-mail: agneeshwari@gmail.com

Forced convective heat and mass transfer flow of hydromagnetic, radiating and dissipative fluid over a porous nonlinear stretching sheet in the presence of non-uniform heat generation/absorption is investigated numerically. The system of nonlinear partial differential equations governing the physical problem is reduced to nonlinear ordinary differential equations by means of suitable similarity transformations and are solved numerically using Nachtsheim Swigert shooting iteration scheme together with fourth order Runge Kutta method. The effects of various physical parameters on velocity, temperature and concentration distributions are depicted graphically. The important findings of this study exhibited that the effect of non-uniform heat generation/absorption parameter and radiation parameter have significant role in controlling thermal boundary layer thickness and temperature. Numerical values of the skin friction coefficient, temperature and concentration at the wall are shown in a tabular form. A comparison is made with previously published data which results in good agreement.

Key words: MHD, heat flux, mass flux, non-uniform heat generation/absorption.

1. Introduction

In recent years, considerable attention has been paid to the study of boundary layer flow over a porous surface due to its importance in the engineering and practical life such as manufacturing technology, agriculture, ceramics and metallurgy process, engineering and soil mechanics. Further, investigations of laminar boundary-layer flow and heat transfer of an incompressible fluid over a nonlinear stretching surface has attracted the attention of many researchers due to their applications over a broad spectrum of science and technology disciplines, such as wire and fiber coating, aerodynamic extrusion of plastic sheets, cooling of metallic plates, drawing of polymer sheets, annealing and thinning of copper wires.

Sakiadis [1a, b] initiated the study of boundary layer flow over a continuous solid surface moving with constant speed. This problem has been extensively studied by taking into account various combinations. Crane [2] studied the boundary layer flow past a stretching sheet and he obtained a closed form solution. Hydromagnetic flow over a stretching sheet with heat transfer of a constant surface temperate was discussed by Chakrabarti and Gupta [3]. Gupta and Gupta [4] extended this problem for the case in the presence of suction or blowing at the moving surface. Ali [5] investigated the thermal boundary layer flow by

* To whom correspondence should be addressed

considering the nonlinear stretching surface. The flow and heat transfer over a stretching surface under various physical situations have been analysed by many researchers. Chiam [6] examined the numerical solution of MHD flow and heat transfer over a nonlinear stretching surface with power law velocity. Heat transfer over a nonlinear stretching surface with variable surface heat flux was studied by Elsayed and Elbashbeshy [7]. Anjali Devi and Ganga [8] analysed MHD nonlinear flow and heat transfer over a stretching porous surface of constant heat flux.

In a physical situation which deals with high temperatures, the role of thermal radiation effect on flow and heat transfer processes is important a Raptis and Massalas [9] discussed MHD flow over a flat plate in the presence of radiation. Raptis *et al*. [10] investigated the numerical solution of the flow field with the influence of both the magnetic field and radiation. Abbas and Hayat [11] analysed the radiation effects on MHD flow in a porous space.

The study of boundary layer problems with heat transfer, taking into consideration dissipation effects, adds a new dimension to it. Gebhart [12] was the first who analysed viscous dissipation effects in natural convection. Heat transfer in a viscous fluid over a stretching sheet with viscous dissipation and internal heat generation was studied by Vajravelu and Hadjinicolaou [13]. Cortell [14] studied the effects of radiation and viscous dissipation on the thermal boundary layer over a nonlinearly stretching sheet with PST and PHF case. Bataller [15] analysed the boundary layer flow and heat transfer with thermal radiation. Dissipation effects on nonlinear MHD flow over a stretching surface with prescribed heat flux were analysed by Anjali Devi and Ganaga [16]. Recently, Jamaludin *et al*. [17] investigated the numerical solution of heat transfer past a stretching sheet with viscous dissipation and internal heat generation with prescribed surface temperature.

However, the effects of non-uniform heat generation/absorption on the flow and heat transfer have not been taken into account in most of the investigations. The effect of non-uniform heat generation or absorption is more important in several physical problems such as fluids undergoing exothermic or endothermic process. The blowing/suction effect on hydromagnetic heat transfer by mixed convection from an inclined continuously stretching surface with non-uniform internal heat source/sink was first studied by Abo-Eldahab and El Aziz [18] and later the effects of non-uniform heat generation/absorption were analysed by several investigators under various physical situations. Recently, Anjali Devi *et al*. [19] investigated the effects of radiation on MHD flow over a non-linearly stretching sheet with non- uniform heat source/sink.

Combined heat and mass transfer ensues in many processes such as absorption, evaporation, drying, precipitation, membrane filtration and distillation. So it is necessary to investigate such combined features of momentum, heat and mass transfer in laminar flow over a porous nonlinear stretching surface. Ganga and Anjali Devi [20] analysed the hydromagnetic flow with heat and mass transfer over a stretching porous surface with prescribed heat, mass flux and viscous dissipation effects. Anjali Devi and Kayalvizhi [21] studied the nonlinear hydromagnetic flow with radiation and heat source over a stretching surface with prescribed heat and mass flux embedded in a porous medium. Jat *et al*. [22] discussed heat and mass transfer for viscous flow over a nonlinearly stretching sheet in a porous medium. Effects of radiation and partial slip on heat and mass fluxes of viscous dissipative flow over a stretching sheet were examined by Kayalvizhi *et al*. [23].

Motivated by the investigations and applications mentioned above, the main objective of this analysis is to study the effects of heat and mass fluxes and non-uniform heat generation/absorption on hydromagnetic flow over a porous nonlinear stretching surface in the presence of thermal radiation and viscous dissipation. Using similarity transformations, the governing nonlinear partial differential equations are transformed into a system of nonlinear ordinary differential equations and then are solved numerically using the Nachtsheim Swigert shooting iteration technique along with the fourth order Runge-Kutta integration method.

2. Mathematical formulation

Consider a steady, laminar, two-dimensional hydromagnetic flow of a viscous, incompressible electrically conducting and radiating fluid over a porous nonlinear stretching surface in the presence of non-

uniform heat generation/absorption and viscous dissipation with prescribed heat and mass fluxes. The flow is generated due to stretching of the surface that is caused by a simultaneous application of two equal and opposite forces along the *x*-axis. Keeping the origin fixed, the surface stretches non-linearly with the velocity $u_w(x)$.The flow is assumed to be in the *x*-direction, which is chosen along the surface and the *y*-axis is perpendicular to it and *u* and *v* are the fluid tangential velocity and normal velocity, respectively. A transverse magnetic field $\boldsymbol{B}$ is applied to the sheet.

The magnetic Reynolds number R_m is assumed to be small and hence when $R_m << 1$, the induced magnetic field is assumed to be negligible in comparison to that of the imposed magnetic field [cf. Davidson [24]]. Since the flow is steady, curl $\boldsymbol{E} = 0$ and also div $\boldsymbol{E} = 0$ in the absence of surface charge density. Hence $\boldsymbol{E} = 0$ and it is also assumed that the electric field due to polarization of charges is negligible. The fluid is considered to be a gray, absorbing, emitting radiation but non-scattering medium. The radiative heat flux in the *x*-direction is considered to be negligible in comparison to that in the *y*-direction and the boundary layer approximations are made. The Rosseland approximation is used in the energy equation to describe the radiative heat flux. The flow configuration and the co-ordinate system are shown in Fig.1.

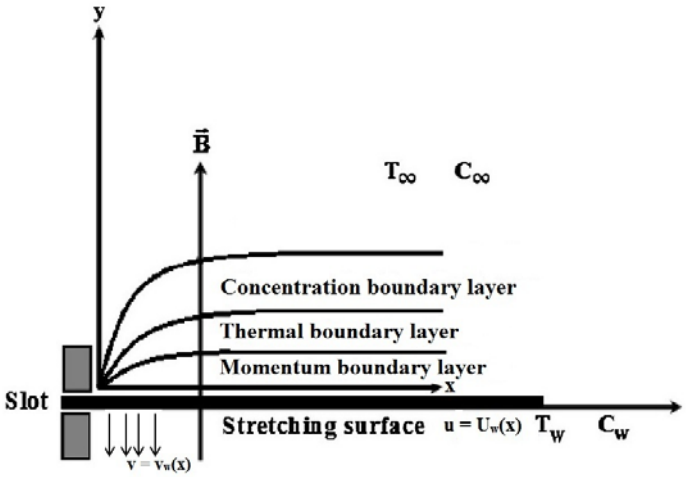

Fig.1. Schematic diagram.

The governing equations of the problem under consideration are given in [14]

$$\frac{\partial u}{\partial x}+\frac{\partial v}{\partial y}=0, \tag{2.1}$$

$$u\frac{\partial u}{\partial x}+v\frac{\partial u}{\partial y}=\nu\frac{\partial^2 u}{\partial y^2}-\frac{\sigma B^2}{\rho}u, \tag{2.2}$$

$$u\frac{\partial T}{\partial x}+v\frac{\partial T}{\partial y}=\frac{k}{\rho C_p}\frac{\partial^2 T}{\partial y^2}+\frac{q'''}{\rho C_p}-\frac{1}{\rho C_p}\frac{\partial q_r}{\partial y}+\frac{\mu}{\rho C_p}\left(\frac{\partial u}{\partial y}\right)^2, \tag{2.3}$$

$$u\frac{\partial C}{\partial x}+v\frac{\partial C}{\partial y}=D\frac{\partial^2 C}{\partial y^2} \tag{2.4}$$

where k is the thermal conductivity, σ is the electrical conductivity, ρ is the density, μ is the viscosity, ν is the kinematic viscosity, T is the flow temperature, C is the fluid concentration, C_p is the specific heat at constant pressure, D is the coefficient of mass diffusivity. In order to obtain a similarity solution, a special form of the magnetic field such as $B = B_0 x^{\frac{n-1}{2}}$ is chosen following Chiam [6] where B_0 is the constant magnetic field, and q''' is the non-uniform heat generation/absorption [non-uniform heat source/sink] defined as [18]

$$q''' = \frac{k\, u_w(x)}{x\,\nu}\left(A^* \left(T_w - T_\infty\right) e^{-\eta} + B^* \left(T - T_\infty\right)\right) \tag{2.5}$$

where $u_w(x) = bx^n$, b is a constant, n is the power-law index, T_w is the temperature of the wall, A^* and B^* are exponentially decaying parameters of space and temperature dependent internal heat generation/absorption respectively. Here $A^* > 0$ and $B^* > 0$ correspond to internal heat generation while $A^* < 0$ and $B^* < 0$ correspond to internal heat absorption. The Rosseland approximation [10] for the radiation heat flux is given by

$$q_r = -\frac{4\sigma^*}{3k^*}\frac{\partial T^4}{\partial y} \tag{2.6}$$

where σ^* and k^* are the Stephan-Boltzman constant and Rosseland mean absorption coefficient. It is assumed that [15] the temperature differences within the flow are such that the term T^4 may be expressed as a linear function of temperature. Expanding T^4 using the Taylor series and neglecting higher order terms yields

$$T^4 \cong 4T_\infty^3 T - 3T_\infty^4. \tag{2.7}$$

Substituting Eqs (2.6) and (2.7) in Eq.(2.3) we have

$$u\frac{\partial T}{\partial x} + v\frac{\partial T}{\partial y} = \frac{k}{\rho C_p}\frac{\partial^2 T}{\partial y^2} + \frac{q'''}{\rho C_p} + \frac{16\,\sigma^* T_\infty^3}{3k^*\,\rho C_p}\frac{\partial^2 T}{\partial y^2} + \frac{\mu}{\rho C_p}\left(\frac{\partial u}{\partial y}\right)^2. \tag{2.8}$$

The appropriate boundary conditions are

$$\begin{gathered} u_w(x) = bx^n,\ \ v = -v_w(x),\quad q_w = -k\frac{\partial T}{\partial y} = E_0 x^r,\quad m_w = -D\frac{\partial C}{\partial y} = E_1 x^m,\ \ \text{at}\ \ y = 0, \\ u = 0,\qquad T = T_\infty,\qquad C = C_\infty\qquad \text{as}\qquad y \to \infty. \end{gathered} \tag{2.9}$$

Here $v_w(x) = S\sqrt{\frac{b\nu(n+1)}{2}}\, x^{\frac{n-1}{2}}$ is the suction velocity where S is a constant ($S > 0$), E_0 and E_1 are constants, r is the heat flux exponent, m is the mass flux exponent, T_∞ is the temperature of the ambient fluid, C_∞ is the concentration of the ambient fluid.

3. Similarity transformations

The mathematical analysis of the problem is simplified by introducing the following dimensionless variables *f* and the similarity transformations which are defined by Cortell [14]

$$\psi(x,y)=\sqrt{\frac{2b\nu}{n+1}x^{n+1}}f(\eta),\qquad \eta(x,y)=y\sqrt{\frac{b(n+1)}{2\nu}}x^{\frac{n-1}{2}},$$
$$T-T_\infty=\frac{E_0}{k}x^{2n}\sqrt{\frac{2\nu}{b(n+1)}}\theta(\eta),\qquad C-C_\infty=\frac{E_1}{D}x^{2n}\sqrt{\frac{2\nu}{b(n+1)}}\varphi(\eta). \tag{3.1}$$

The stream function ψ satisfies the continuity Eq.(2.1). The velocity component $f'(\eta)$, dimensionless temperature $\theta(\eta)$ and dimensionless concentration $\varphi(\eta)$ are given by

$$u=\frac{\partial\psi}{\partial y}=bx^n f'(\eta),\qquad v=-\frac{\partial\psi}{\partial x}=-\sqrt{\frac{b\nu(n+1)}{2}}x^{\frac{n-1}{2}}\left(f(\eta)+\frac{n-1}{n+1}\eta f'(\eta)\right),$$
$$\theta(\eta)=\frac{T-T_\infty}{T_w-T_\infty},\qquad \varphi(\eta)=\frac{C-C_\infty}{C_w-C_\infty} \tag{3.2}$$

where $T_w-T_\infty=\frac{E_0}{k}x^r\sqrt{\frac{2\nu}{b(n+1)}}x^{\frac{1-n}{2}}$, $C_w-C_\infty=\frac{E_1}{D}x^m\sqrt{\frac{2\nu}{b(n+1)}}x^{\frac{1-n}{2}}$, $r=\frac{5n-1}{2}$ and $m=\frac{5n-1}{2}$.

Employing the transformations (3.1) and (3.2), the nonlinear partial differential Eqs (2.2)-(2.4) are transformed to the following nonlinear ordinary differential equations [14]

$$f'''+ff''-\frac{2n}{n+1}f'^2-M^2f'=0, \tag{3.3}$$

$$\theta''+\frac{2k_0}{n+1}\left(A^*e^{-\eta}+B^*\theta\right)+\Pr k_0 f\theta'-\Pr\frac{4n}{n+1}k_0f'\theta+\Pr\mathrm{Ec}\,k_0f''^2=0, \tag{3.4}$$

$$\phi''+\mathrm{Sc}\,f\phi'-\frac{4n}{n+1}\mathrm{Sc}\,f'\varphi=0. \tag{3.5}$$

The corresponding boundary conditions are

$$f(0)=S,\quad f'(0)=1,\quad \theta'(0)=-1,\quad \varphi'(0)=-1\quad \text{at}\quad \eta\to 0,$$
$$f'(\eta)\to 0,\quad \theta(\eta)\to 0,\quad \varphi(\eta)\to 0,\quad \text{as}\quad \eta\to\infty \tag{3.6}$$

where $M^2 = \frac{2\sigma B_0^{\,2}}{\rho b(n+1)}$ is the magnetic interaction parameter.

$k_0 = \left(\frac{3N_R}{3N_R+4}\right)$, $N_R = \frac{kk^*}{4\sigma^* T_\infty^3}$ is the radiation parameter.

$\mathrm{Pr} = \frac{\nu}{\alpha}$ is the Prandtl number .

$S = \frac{v_w(x)}{\sqrt{\frac{b\nu(n+1)}{2}}\, x^{\frac{n-1}{2}}}$ is the suction parameter.

$\mathrm{Ec} = \frac{k\,b^2}{E_0\, C_p}\sqrt{\frac{b(n+1)}{2\nu}}$ is the Eckert number.

$\mathrm{Sc} = \frac{\nu}{D}$ is the Schmidt number.

The important physical quantities of interest are the skin friction coefficient, Nusselt number and Sherwood number which are defined as

$$C_f = \frac{2\tau_w}{\rho u_w^{\,2}}, \qquad \mathrm{Nu}_x = \frac{x q_w}{k(T_w - T_\infty)} \quad \text{and} \quad \mathrm{Sh}_x = \frac{x\, m_w}{D_m(C_w - C_\infty)} \tag{3.7}$$

where the wall shear stress τ_w, the surface heat flux q_w and mass flux at the surface m_w are given by

$$\tau_W = \mu\left(\frac{\partial u}{\partial y}\right)_{y=0}, \quad q_W = \left(-k\frac{\partial T}{\partial y} + q_r\right)_{y=0} \quad \text{and} \quad m_W = -D_m\left(\frac{\partial C}{\partial y}\right)_{y=0}. \tag{3.8}$$

Substituting Eq.(3.8) in Eq.(3.7), the skin friction coefficient, local Nusselt number and Sherwood number are obtained as

$$\sqrt{\mathrm{Re}_x}\, C_f = \sqrt{2(n+1)}\, f''(0), \tag{3.9}$$

$$\frac{\mathrm{Nu}_x}{\sqrt{\mathrm{Re}_x}} = \left(\frac{3N_R + 4}{3N_R}\right)\sqrt{\frac{n+1}{2}}\,\frac{1}{\theta(0)}, \tag{3.10}$$

$$\frac{\mathrm{Sh}_x}{\sqrt{\mathrm{Re}_x}} = \sqrt{\frac{n+1}{2}}\,\frac{1}{\varphi(0)} \tag{3.11}$$

where $\mathrm{Re}_x = \frac{u_w x}{\nu}$ is the local Reynolds number

4. Numerical solution

The set of administering Eqs (3.3)-(3.5) with boundary conditions (3.6) constitute a highly nonlinear boundary value problem of third order in f and second orders in θ and ϕ. Since the exact solution does not seem to be feasible for the system of nonlinear equations, a numerical solution is sought. The nonlinear boundary value problem is converted into a nonlinear initial value problem using the prominent shooting method, namely, the Nachtsheim Swigert [25] shooting iteration scheme to satisfy asymptotic boundary conditions. The resulting initial value problem is solved using the Runge Kutta fourth order technique for different values of the physical parameters.

The suitable guess values for $f''(0), \theta(0)$ and $\phi(0)$ are obtained using the Nachtsheim Swigert iteration technique and later initial value problems are solved with the assistance of the classical fourth order Runge Kutta method. The step size $h = 0.01$ is employed to obtain the numerical solutions with five decimal place accuracy as a criterion of convergence. The convergence criterion is based on the difference of the present and the previous iteration values which matches up to a tolerance of 10^{-5} and the choice of $\eta_{max}= 7$ confirmed that entire numerical results approached the pertinent asymptotic values. The numerical solutions are obtained for various values of the physical parameters for the flow field, dimensionless temperature and concentration distributions. Numerical values of the skin friction coefficient, temperature and concentration at the wall are also achieved.

5. Results and discussion

A numerical solution of the physical problem is sought for different values of the physical parameters in order to have a clear physical insight into the problem. The effects of various physical parameters such as the magnetic interaction parameter, power-law index, suction parameter, Prandtl number, space dependent heat generation/absorption parameter, temperature dependent heat generation/absorption parameter, radiation parameter, Eckert number and Schmidt number are displayed graphically through Figs 2-16a.

In order to verify the validity and accuracy of the numerical computations, a comparison of the present results with earlier published data has been made and the results are displayed through Tab.1. A comparative study of the skin friction coefficient for different values of n in the absence of the magnetic interaction parameter ($M^2 = 0$) and suction parameter ($S = 0$) with the existing results of Cortell [14] elucidates the fact that the present results are in excellent agreement with these of Cortell [14] which also validate the accuracy of numerical computations.

Table 1. Comparative study of $f''(0)$ for various values of n.

n	$f''(0)$	
	Cortell [14]	Author's result
0.1	*0.705897*	*0.705925*
0.3	*0.815696*	*0.815714*
0.6	*0.918172*	*0.918178*
0.9	*0.983242*	*0.983247*
1.0	*1.000000*	*1.000000*
1.5	*1.061587*	*1.061601*
3.0	*1.148588*	*1.148593*
10.0	*1.234875*	*1.234875*

Further, the wall temperature $\theta(0)$ for various values of the power-law index, radiation parameter, Prandtl number and Eckert number in the absence of $A^*=0$, $B^*=0$ and $S=0$ is compared with this reported by Cortell [14] which is displayed through Tab.2 and it is noted that the results are found to be in good agreement.

Table 2. Comparative study of wall temperature $\theta(0)$ for various values of n, Pr, N_R and Ec when $A^*= 0$, $B^*= 0$ and $S = 0$.

n	Pr	N_R	E_C	$\theta(0)$	
				Cortell [14]	Author's result
1.5	*1.0*	*1.0*	*0.1*	*1.210117*	*1.210060*
3.0				*1.092587*	*1.092590*
10.0				*0.998433*	*0.998432*
1.5	*1.0*	*1.0*	*0.1*	*1.210117*	*1.210005*
	2.0			*0.786038*	*0.785907*
	5.0			*0.473743*	*0.473736*
1.5	*2.0*	*1.0*	*0.1*	*0.786038*	*0.785907*
		2.0		*0.647865*	*0.647834*
		5.0		*0.557023*	*0.557001*
1.5	*2.0*	*1.0*	*0.05*	*0.774378*	*0.774374*
			0.1	*0.786038*	*0.785907*
			0.5	*0.878262*	*0.878262*

Figure 2 illustrates the influence of the magnetic field on the dimensionless velocity distribution. It is clearly noted that the effect of the magnetic field retards the velocity at all points of the flow field. Since the applied magnetic field produces a drag in the form of Lorentz force, which opposes the flow field, the velocity and momentum boundary layer thickness diminish in magnitude with the increase of the magnetic interaction parameter.

The dimensionless velocity for different values of the power-law index n is plotted in Fig.3. An increasing value of the power-law index is to reduce the dimensionless velocity and momentum boundary layer thickness. However, this effect is less significant. Figure 4 shows the effect of the suction parameter S on the dimensionless velocity distribution. It is noted that the velocity decelerates with increasing values of the suction parameter, which also leads to a reduction in momentum boundary layer thickness.

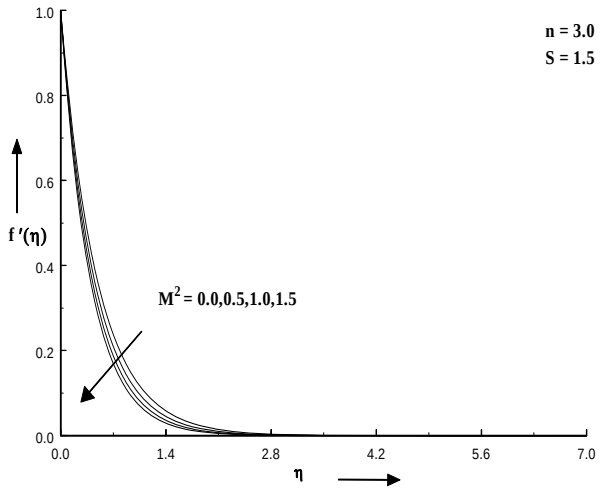

Fig.2. Dimensionless velocity profiles for different values of M^2.

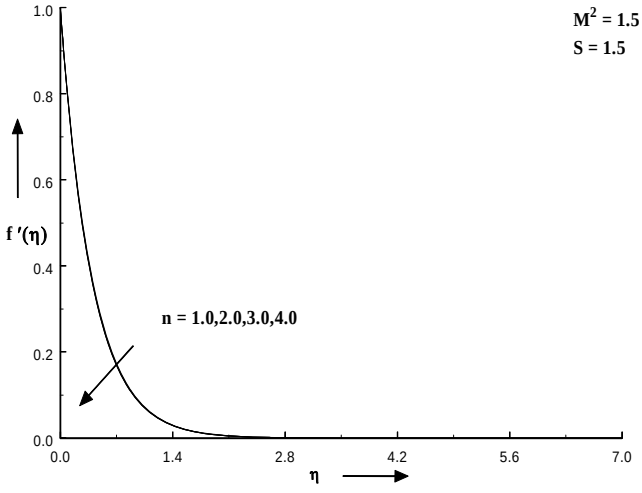

Fig.3. Dimensionless velocity profiles for different values of n.

The effect of the magnetic field on the dimensionless temperature distribution is depicted in Fig.5. The effect of the magnetic field has the tendency to enhance the temperature and thermal boundary layer

thickness. This happens due to Lorentz force, which produces a considerable amount of frictional heating. Further, the increase in the magnetic interaction parameter leads to thickening of the thermal boundary layer. The dimensionless temperature distribution for different values of the power-law index n is exhibited in Fig.6. It is noted that an increase in n leads to a decline in temperature.

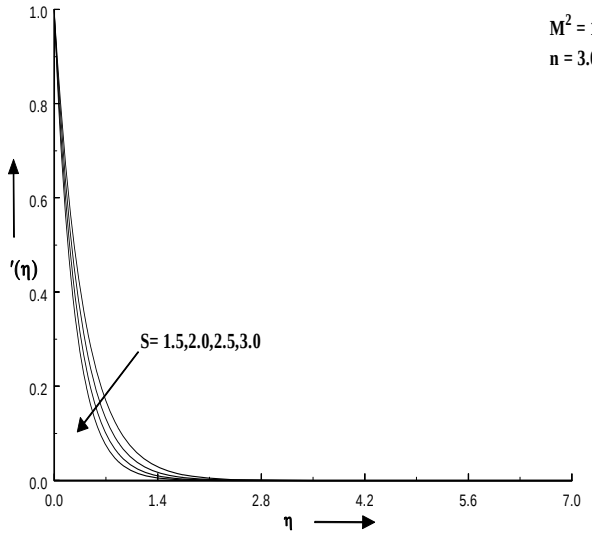

Fig.4. Dimensionless velocity profiles for different values of S.

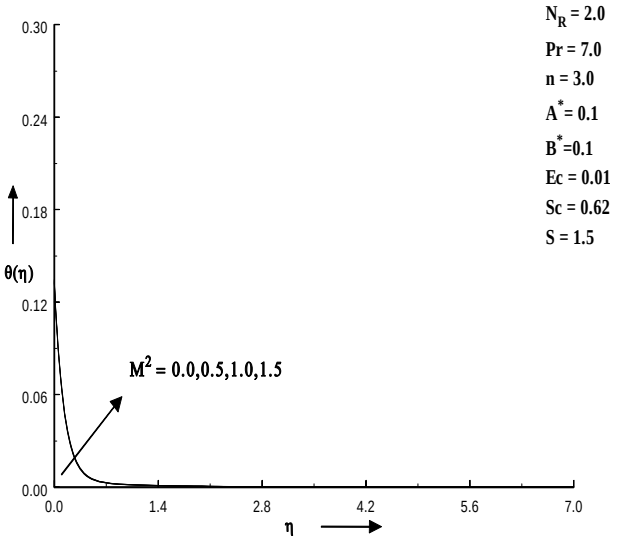

Fig.5. Temperature distribution for different values of M^2.

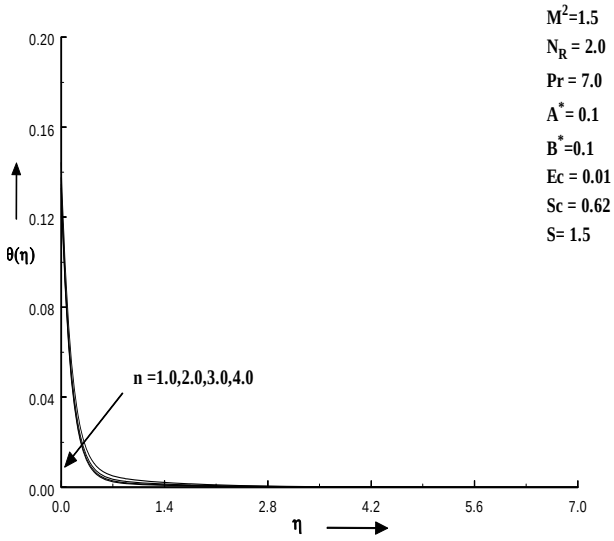

Fig.6. Effect of n on the temperature distribution.

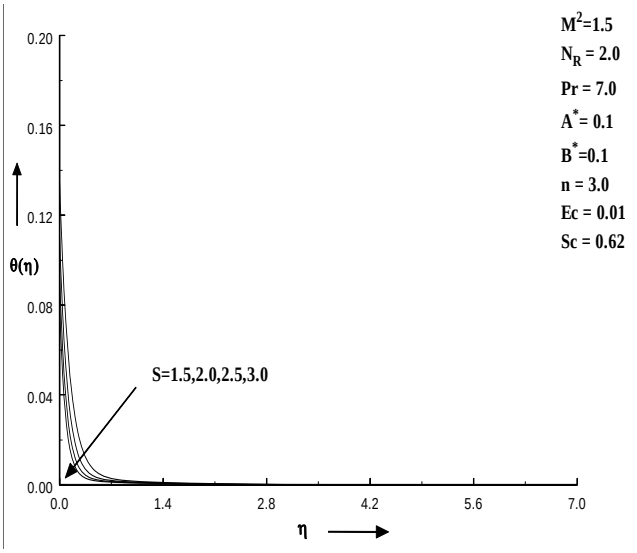

Fig.7. Temperature distribution for different values of S.

The influence of the power-law index on the thermal boundary layer thickness becomes less significant. Figure 7 illustrates the impact of the suction parameter S on the dimensionless temperature distribution. This implies that the temperature and thermal boundary thickness decrease for increasing values of the suction parameter. Figure 8 describes the salient effect of the Prandtl number Pr on the dimensionless temperature distribution. As the value of the Prandtl number increases, both the temperature and thermal

boundary layer thicknesses get decreased due to the lowering of thermal conductivity. Henceforth, the Prandtl number controls the relative thickness of the thermal boundary layer. The influence of the space dependent heat generation/absorption parameter A^* on the temperature distribution is shown in Fig.9. It is observed that energy is created in the boundary layer for increasing values of the heat generation parameter A^* ($A^* > 0$). Physically, exothermic reactions which ensued in the system and a significantly large amount of heat increase the temperature distribution of the fluid. In case of heat absorption ($A^* < 0$), energy was absorbed in the boundary layer, hence the temperature reduces considerably with the increasing values of heat absorption.

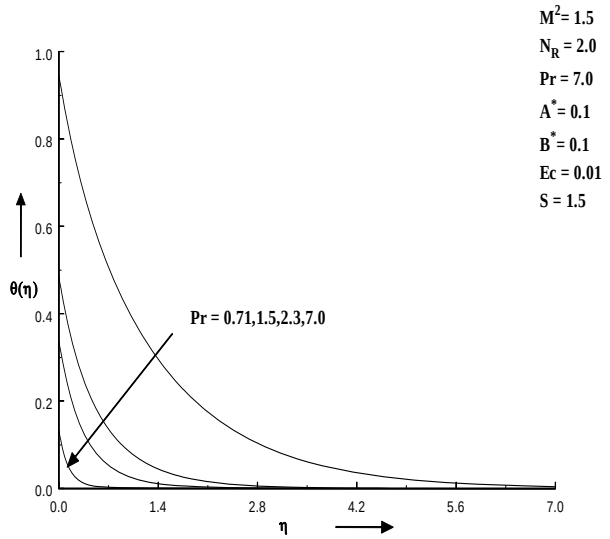

Fig.8. Temperature distribution for different values of Pr.

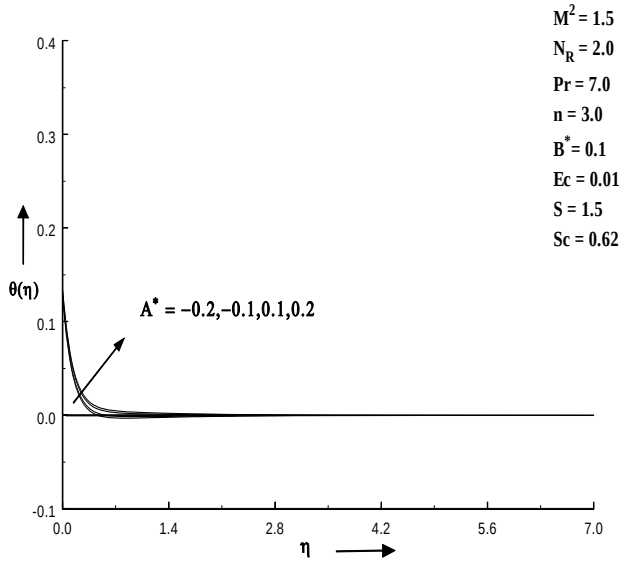

Fig.9. Effect of A^* on the temperature distribution.

Figure 10 depicts the impact of the temperature dependent heat generation/absorption parameter B^* on the dimensionless temperature. Energy is produced in the boundary layer for increasing values of the temperature dependent heat generation parameter B^* ($B^* > 0$). Hence the thermal boundary layer thickness increases. While in the presence of heat absorption $B^* < 0$, energy is absorbed for increasing values of B^*. Hence, the thermal boundary layer thickness as well as the temperature decrease.

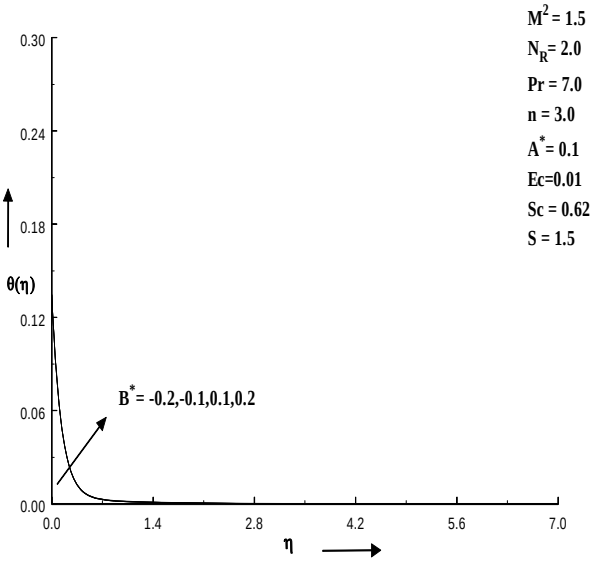

Fig.10. Temperature distribution for different values of B^*.

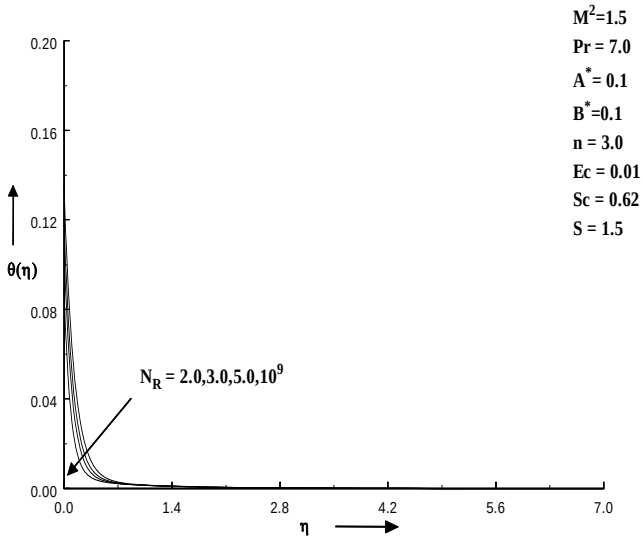

Fig.11. Temperature distribution for different values of N_R.

The effect of the radiation parameter N_R on the dimensionless temperature is illustrated in Fig.11. When the value of the radiation parameter is amplified, the temperature declines and consequently the thermal boundary layer thickness become smaller. This is consistent with the well-known fact that the thermal boundary layer thickness decreases rapidly with increasing values of the radiation parameter. Figure 12 demonstrates the dimensionless temperature distribution for different values of the Eckert number Ec. Increasing values of the Eckert number cause the storage of energy in the fluid region as a result of dissipation which is caused by viscosity thus creating heat due to frictional heating. It reveals that increasing values of the Eckert number upgrade the temperature as well as the thermal boundary layer thickness.

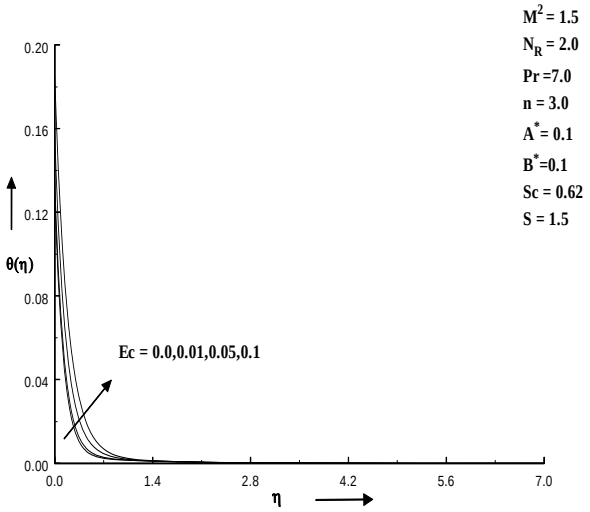

Fig.12. Temperature distribution for different values of Ec.

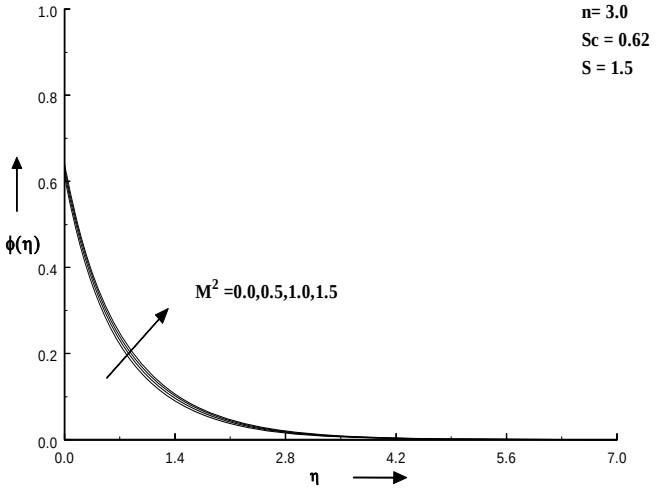

Fig.13. Concentration distribution for different values of M^2.

Figure 13 elucidates the effect of the magnetic field on the dimensionless concentration distribution. An increase in the magnetic interaction parameter enhances the dimensionless concentration and the thickness of concentration boundary layer. The influence of the power-law index n on the dimensionless concentration is shown in Fig.14. It is noticed that the concentration distribution and concentration boundary layer thickness decrease with an increase of the power law index n.

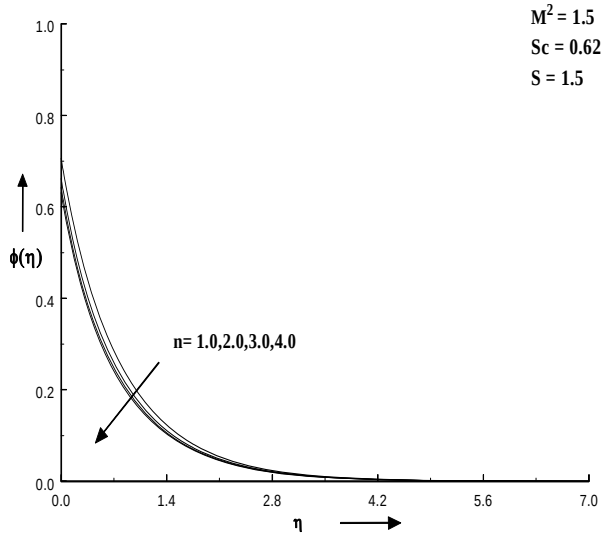

Fig.14. Concentration distribution for different values of n.

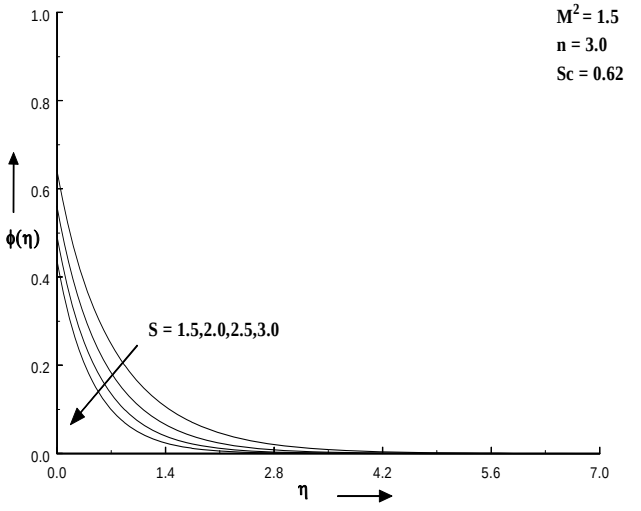

Fig.15. Concentration distribution for different values of S.

The dimensionless concentration distribution for various values of the suction parameter S is illustrated in Fig.15. It is clear that the suction parameter reduces the dimensionless concentration and also boundary layer thickness for its increasing values. Figure 16 shows the concentration distribution for different values of the Schmidt number Sc. It is observed that the effect of the Schmidt number is to decrease the dimensionless concentration. Since an increase in the Schmidt number results in an increase of the viscous diffusion rate, it reduces the concentration boundary layer thickness. To reveal the convergence part, Fig.16a is presented.

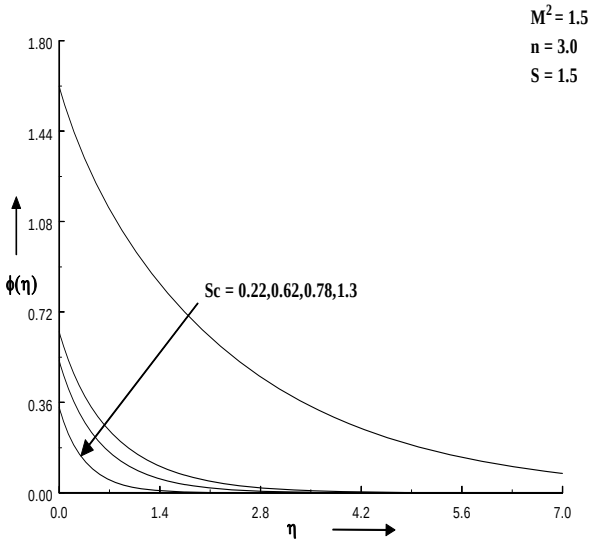

Fig.16. Concentration distribution for different values of Sc.

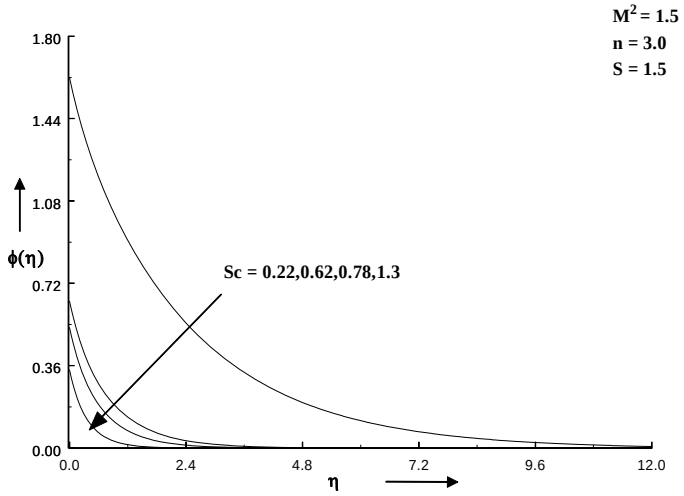

Fig.16a. Effect of Sc on concentration distribution.

The numerical results of the skin friction coefficient for various values of the magnetic interaction parameter, power-law index and suction parameter are given in Tab.3 and it is seen that the skin friction coefficient increases in magnitude for their increasing values.

Table 3. Skin friction coefficient for various values of M^2, n and S.

M^2	n	S	$-f''(0)$	$-\sqrt{2(n+1)}f''(0)$
0.0	*3.0*	*1.5*	*2.10472*	*5.95299*
0.5			*2.28050*	*6.45017*
1.0			*2.43744*	*6.89406*
1.5			*2.58065*	*7.29911*
1.5	*1.0*	*1.5*	*2.50000*	*7.07100*
	2.0		*2.55408*	*7.22396*
	3.0		*2.58065*	*7.29911*
	4.0		*2.59644*	*7.34377*
1.5	*3.0*	*1.5*	*2.58065*	*7.29911*
		2.0	*2.94438*	*8.32788*
		2.5	*3.33252*	*9.42570*
		3.0	*3.74046*	*10.5795*

Table 4 depicts the numerically computed values of the non-dimensional rate of heat transfer for different values of the physical parameters M^2, n, S, Pr, A^*, B^*, N_R and Ec. The dimensionless rate of heat transfer gets enhanced for increasing values of the power-law index, suction parameter, Prandtl number, non-uniform heat sink ($A^* < 0$, $B^* < 0$) parameter. However, this trend is reversed for increasing values of the magnetic interaction parameter, Eckert number, radiation parameter and non-uniform heat source ($A^* > 0$, $B^* > 0$) parameter.

Table 4. Nusselt number for various values of M^2, n, S, Pr, A^*, B^*, N_R and Ec.

Physical parameters	$\theta(0)$	$\left(\frac{3N_R+4}{N_R}\right)\sqrt{\frac{n+1}{2}}\frac{1}{\theta(0)}$
$M^2 = 0.0$	0.88854	2.65272
0.5	0.91073	2.58809
1.0	0.92989	2.53476
1.5	0.94684	2.48938
$n = 1.0$	1.12761	1.47808
2.0	0.99929	2.04266
3.0	0.94684	2.48938
4.0	0.91831	2.86964
$S = 1.5$	0.94684	2.48938
2.0	0.83049	2.83814
2.5	0.73406	3.21097
3.0	0.65420	3.60295
Pr = 0.71	0.94684	2.48938
1.5	0.48593	4.85059
2.3	0.33858	6.96157
7.0	0.13461	17.51019
$A^* = -0.2$	0.87232	2.70204
-0.1	0.89717	2.62720
0.1	0.94684	2.48938
0.2	0.97168	2.42574
$B^* = -0.2$	0.87628	2.68983
-0.1	0.89693	2.62791
0.1	0.94684	2.48938
0.2	0.97822	2.40953
$N_R = 2.0$	0.94684	2.48923
3.0	0.83505	2.44617
5.0	0.74557	2.40249
10^9	0.61072	2.31563
Ec = 0.0	0.94213	2.50183
0.01	0.94684	2.48938
0.05	0.96571	2.44074
0.1	0.98930	2.38254

Table 5 shows the numerical results of the non-dimensional rate of mass transfer for various values of the magnetic interaction parameter, power-law index, suction parameter and Schmidt number. The non-dimensional rate of mass transfer is reduced for increasing values of M^2 and enhanced for increasing values of n, S and Sc.

Table 5. Sherwood number for various values of M^2, n, S and Sc.

M^2	n	S	Sc	$\varphi(0)$	$\sqrt{\frac{n+1}{2}}\frac{1}{\varphi(0)}$
0.0	*3.0*	*1.5*	*0.62*	*0.61420*	*2.30251*
0.5				*0.62493*	*2.26297*
1.0				*0.63423*	*2.22979*
1.5				*0.64250*	*2.20109*
1.5	*1.0*	*1.5*	*0.62*	*0.70606*	*1.41631*
	2.0			*0.66195*	*1.85014*
	3.0			*0.64250*	*2.20109*
	4.0			*0.63155*	*2.50352*
1.5	*3.0*	*1.5*	*0.62*	*0.64250*	*2.20109*
		2.0		*0.56103*	*2.52072*
		2.5		*0.49384*	*2.86368*
		3.0		*0.43853*	*3.22486*
1.5	*3.0*	*1.5*	*0.22*	*1.61979*	*0.87308*
			0.62	*0.64250*	*2.20109*
			0.78	*0.52732*	*2.68186*
			1.3	*0.34194*	*4.13581*

6. Conclusion

In this paper, numerical investigation has been carried out to analyse hydromagnetic heat and mass transfer flow of an electrically conducting and radiating fluid over a porous nonlinear stretching surface with prescribed heat and mass fluxes in the presence of non-uniform heat generation/absorption and viscous dissipation. Numerical results are obtained for various values of physical parameters and their effects on the flow field, temperature and concentration distributions as well as on the skin friction co-efficient, non-dimensional rate of heat and mass transfer are analysed. The numerical results are found to be in excellent agreement with those of Cortell [14], justifying the adopted numerical scheme. On the basis of the above study, the following observations are made:

- The effect of the magnetic field declines the momentum boundary layer thickness, non-dimensional rate of heat and mass transfer whereas it enhances the dimensionless temperature, concentration and skin friction co-efficient in magnitude. The velocity and temperature of the hydromagnetic flow can be controlled by suitably regulating the strength of the external magnetic field.
- The power-law index decelerates the dimensionless velocity, reduces the temperature and concentration distributions whereas it enhances the non-dimensional rate of heat and mass transfer and skin friction co-efficient in magnitude.
- The radiation parameter and Prandtl number diminish both the temperature and thermal boundary layer thickness. The non-dimensional rate of heat transfer is enhanced by the Prandtl number whereas the effect of the radiation parameter is to suppress it.
- The suction parameter has the tendency to reduce the velocity, temperature, concentration boundary layer thickness while, it enhances the skin friction co-efficient in magnitude and the non-dimensional rate of heat and mass transfer.
- The energy dissipation due to viscosity broadens the thermal boundary layer thickness but it decreases the non-dimensional rate of heat transfer.
- The space dependent heat generation parameter A^* ($A^* > 0$) and temperature dependent heat generation parameter B^* ($B^*>0$) increase the thermal boundary layer thickness as well as the temperature, while the space dependent heat absorption ($A^*<0$) and temperature dependent heat

absorption ($B^*<0$) have the opposite effect to reduce both the temperature and thermal boundary layer thickness. It is also noted that the non-dimensional rate of heat transfer decreases for increasing heat generation parameter whereas it enhances due to heat absorption parameter for its increasing values.

- The Schmidt number has a significant influence on the concentration boundary layer thickness so as to reduce it, whereas its effects on the non-dimensional rate of mass transfer show an opposite trend. It is worth mentioning that the present study may find applications in space technology, exothermic/endothermic processes, geothermal energy systems and cooling of nuclear reactors.

Nomenclature

A^* – space dependent heat source/sink parameter
B^* – temperature dependent heat source/sink parameter
B_0 – magnetic field strength
b – dimensional constant
C – concentration of the fluid
C_f – skin friction coefficient
C_p – specific heat at constant pressure
C_∞ – concentration of the ambient fluid
D – mass diffusivity coefficient
E_0, E_1 – positive constant
Ec – Eckert number
k – thermal conductivity
k^* – Rosseland mean absorption coefficient
M^2 – magnetic interaction parameter
m_w – mass flux at the surface
Nu_x – Nusselt number
n – power-law index
Pr – Prandtl number
q''' – non-uniform heat source/sink parameter
q_r – radiative heat flux
q_w – surface heat flux
R_d – radiation parameter
Re_x – local Reynolds number
r – heat flux exponent
S – suction parameter
Sc – Schmidt number
Sh_x – Sherwood number
T – fluid temperature
T_w – temperature of the sheet
T_∞ – temperature of the free stream fluid
$v_w(x)$ – suction velocity
β – mass flux exponent
η – similarity variable
μ – viscosity of the fluid
ν – kinematic viscosity of the fluid
ρ – density of the fluid
σ – electrical conductivity of the fluid
σ^* – Stefan Boltzmann constant
τ_w – shear stress at the wall

References

[1] Sakiadis B.C. (1961a): *Boundary layer behavior on continuous solid surface I.* − AICHE Journal, vol.7, pp.26-28.

Sakiadis B.C. (1961b): *Boundary layer behavior on continuous solid surfaces II*, *boundary layer on a continuous flat surface*. − AICHE Journal, vol.**7**, pp.221-225.

[2] Crane L.J. (1970): *Flow past a stretching plate*. − Z Angew Math Physics, vol.21, pp.645-647.

[3] Chakrabarti A. and Gupta A.S. (1979): *Hydromagnetic flow and heat transfer over a stretching sheet*. − Quarterly of Applied Mathematics, vol.37, pp.73-78.

[4] Gupta P.S. and Gupta A.S. (1997): *Heat and mass transfer on a stretching sheet with suction or blowing*. − Canadian Journal of Chemical Engineering, vol.55, pp.744–746.

[5] Ali M.E. (1994): *Analysis on the heat transfer over a continuous stretching surface*. − Wärme und Stofffübertragung, vol. 29, pp.227-234.

[6] Chiam T.C. (1995): *Hydromagnetic flow over a surface stretching with a power- law velocity.* − International Journal of Engineering Science, vol.33, pp.429-435.

[7] Elsayed M.A. and Elbashbeshy (1998): *Heat transfer over a stretching surface with variable surface heat flux*. − Journal of Physics. D Applied Physics, vol.31, pp.1951-1954.

[8] Anjali Devi S.P. and Ganga B. (2008): *MHD nonlinear flow and heat transfer over a stretching porous surface of constant heat flux*. − Computer Assisted Mechanics and Engineering Sciences, vol.15, pp.15-22.

[9] Rapits A. and Massalas C.V. (1998): *Magnetohydrodynamic flow past a plate by the presence of radiation*. − Heat and Mass Transfer, vol.34, pp.107.

[10] Raptis A., Perdikis C. and Takhar H.S. (2004): *Effect of thermal radiation on MHD flow*. − Applied Mathematics and Computation, vol.153, pp.645-49.

[11] Abbas Z. and Hayat T. (2008): *Radiation effect on MHD flow in a porous space*. − International journal of Heat and Mass Transfer, vol.51, No.5, pp.1024-1033.

[12] Gebhart B. (1962): *Effects of viscous dissipation in natural convection.* − Journal of Fluid Mechanics, vol.14, pp.225-232.

[13] Vajravelu K. and Hadjinicolaou A. (1993): *Heat transfer in a viscous fluid over a stretching sheet with viscous dissipation and internal heat generation*. − Internal Communication Heat Mass Transfer, vol.20, No.3, pp.417–30.

[14] Cortell R. (2008): *Effects of viscous dissipation and radiation on the thermal boundary layer over a nonlinearly stretching sheet*. − Physics Letters A, vol.372, No.5, pp.631-636.

[15] Bataller R.C. (2008): *Similarity solutions for boundary layer flow and heat transfer of a FENE-P fluid with thermal radiation*. − Physics Letters A, vol.372, pp.2431-2439.

[16] Anjali Devi S.P. and Ganga B. (2010): *Dissipation effects on MHD nonlinear flow and heat transfer past a porous surface with prescribed heat flux*. − Journal of Applied Fluid Mechanics, vol.3, No.1, pp.1-6.

[17] Jamaludin M.A., Nazar R. and Shafie S. (2017): *Numerical solution of heat transfer past a stretching sheet with viscous dissipation and internal heat generation with prescribed surface temperature*. − AIP Conference Proceedings vol.1830, 020058.

[18] Emad M. Abo-Eldahab and Mohamed A. El Aziz (2004): *Blowing/suction effect on hydromagnetic heat transfer by mixed convection from an inclined continuously stretching surface with internal heat generation/absorption.* − International Journal of Thermal Science vol.43, pp.709-719.

[19] Anjali Devi S.P., Agneeshwari M. and Wilfred Samuel Raj J. (2018): *Radiation effects on MHD boundary layer flow and heat transfer over a nonlinear stretching surface with variable wall temperature in the presence of non-uniform heat source/sink*. – International Journal of Applied Mechanics and Engineering, vol.23, pp.289-305.

[20] Ganga B. and Anjali Devi S.P. (2008): *MHD nonlinear flow with heat and mass transfer over a stretching porous surface with prescribed heat, mass flux and viscous dissipation effects*. – 8th ISHMT-ASME Heat and Mass Transfer Conference, Jawaharlal Nehru Technological University, Hyderabad, India, HMT- 1.

[21] Anjali Devi S.P. and Kayalvizhi M. (2013): *Nonlinear hydromagnetic flow with radiation and heat source over a stretching surface with prescribed heat and mass flux embedded in a porous medium*. – Journal of Applied Fluid Mechanics, vol.6, No.2, pp.157-165.

[22] Jat Gopi Chand R.N. and Dinesh Rajotia (2014): *MHD heat and mass transfer for viscous flow over nonlinearly stretching sheet in a porous medium*. – Thermal Energy and Power Engineering, vol.3, No.1, pp.191-197.

[23] Kayalvizhi M., Kalaivanan R., Vishnu Ganesh N., Ganga B. and Abdul Hakeem A.K. (2016): *Velocity slip effects on heat and mass fluxes of MHD viscous–Ohmic dissipative flow over a stretching sheet with thermal radiation*. – Ain Shams Engineering Journal, vol.7, pp.791-797.

[24] Davidson P.A. (2001): *An Introduction to Magnetohydrodynamics*. – UK: Cambridge University Press.

[25] Nachtsheim P.R. and Swigert P. (1965): *Satisfaction of the asymptotic boundary conditions in numerical solution of the system of non-linear equations of boundary layer type*. – NASA TND-3004.

Received: October 12, 2018

Revised: May 23, 2019